Available online at www.sciencedirect.com
SCIENCE DIRECT®
Chemical Physics Letters 397 (2004) 510–515
CHEMICAL PHYSICS LETTERS
www.elsevier.com/locate/cplett

Ab initio investigation of the atomic charges in the KcsA channel selectivity filter

Mylène Compoint, Christophe Ramseyer, Philippe Huetz *

Laboratoire de Physique Moléculaire, UMR CNRS 6624, Faculté des Sciences et Techniques, Université de Franche-Comté, 16 route de Gray, La Bouloie, 25030 Besançon Cedex, France

Received 6 July 2004; in final form 3 September 2004

Abstract

Ab initio calculations are used to calculate the atomic charges in the selectivity filter part of KcsA potassium channel according to the Merz–Kollman–Singh scheme. On the basis of a long molecular dynamics simulation, we show that these charges deviate significantly from the values usually implemented in the most common force fields. These consequent changes may considerably influence our views on the mechanistics of the potassium diffusion process and give strong evidence that the application of electronically polarizable force fields is necessary.

1. Introduction

The voltage-gated KcsA channel is the K^+ channel from Streptomyces lividans, similar in structure to other K^+ channels, e.g. in vertebrates. It is a highly selective tetrameric protein machinary devoted to potassium ions directional transfer through the cell membrane [1]. This function is essential for e.g. neuron electrical signals generation [2] or heart beat [3]. It is yet difficult to understand how such a mechanism can be as much efficient (flow of ca. 10^7 K^+ ions per channel per s) and selective ($\sim$1 Na^+ ion for at least 10^3 K^+ transported). The recent X-ray structure of a procaryotic KcsA channel shed light on the molecular bases of this process [4], as well as different molecular dynamics (MD) simulations [5–7] and theoretical electrostatics and energetics studies [8–12]. The protein switches between an open and a closed structure, where only the closed one is known precisely, the open one being modeled from site-directed spin labeling and electron paramagnetic resonance spectroscopy data or computational conformation analyses [13,14]. Three main regions participate to the channel K^+ diffusion: the selectivity filter at the outermost part of the cell membrane, a water-filled cavity half way across the membrane, followed by the gate region, a vestibule at the innermost part covered with hydrophobic residues (Fig. 1). Four α-helices point towards the central pocket and are lined up with carbonyls of the peptide bonds, disposed four by four in successive planes, in between which the K^+ ions are stabilized in alternation with single water molecules [8]. Precedent calculations [10,15,16] focused on the mechanism of the concerted motions of potassium and water within the pore by exploring the successive sites S_0 (outer mouth) to S_4 and S_{cav} (cavity) filled by either K^+ ions or water (W) molecules. In a recent paper [16] we have studied the specific sequence K_0, W_1, K_2, W_3, K_4 and K_{cav}, which is a stable configuration of the pore, on the structure at 2.0 Å resolution on a 1.4 ns timescale along the selectivity filter. It will be noted KWKWKK for clarity. The most general situation shows that (i) K_0 interacts with four water molecules and the four oxygen atoms of the Gly79 carbonyls, (ii) K_{cav} is completely

* Corresponding author. Fax: +33 381666475.
E-mail address: philippe.huetz@univ-fcomte.fr (P. Huetz).

0009-2614/$ - see front matter © 2004 Elsevier B.V. All rights reserved.
doi:10.1016/j.cplett.2004.09.033

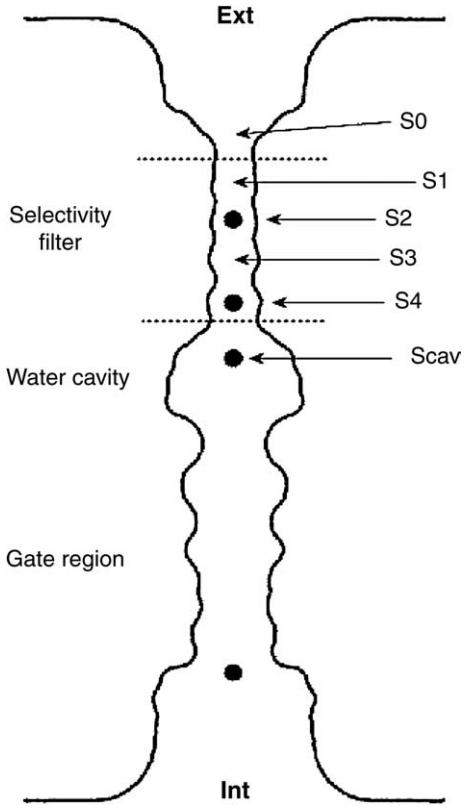

Fig. 1. Schematic representation of the inner KcsA pore space. The different sites (S_0 to S_4, S_{cav}) where the potassium ions (filled black circles) can be located (or water molecules in alternance with K^+) are indicated (here one possible configuration of the K^+ ions). Int: cytoplasmic side, Ext: extracellular side. The part between the two dashed lines (selectivity filter) delimits the truncated model we used in ab initio calculations.

hydrated in the cavity, (iii) K_4 interacts with the four Thr75 carbonyls on one side and with the four oxygen atoms of the hydroxyl groups of the Thr74 aminoacids on the other, whereas (iv) the most stable ion K_2 is surrounded by eight amide carbonyls. Thus, the number of coordinations with oxygens always stays eight, K^+ being progressively dehydrated and rehydrated in this process at the beginning and end of the filter, respectively. The question which can be raised is how K_2, although trapped in a very deep electrostatic well, is further able to diffuse so easily.

Up to now, only effectively polarized force fields like GROMOS, AMBER or CHARMM were applied in biomolecular simulations of ionic channels. In this work, we used the data issued from several snapshots in previous MD simulations on the KcsA channel, performed using the effectively polarized AMBER [17] force field, to calculate Merz–Kollman (MK) charges [18,19] with GAUSSIAN-03 [20] suite of programs. More specifically, we compared one average configuration (C1) over the geometries obtained during 600 MD ps to the situation in a specific case of the atomic positions (C2), within this same trajectory, which is suspected to be at the origin of the 'knock-on' mechanism [21] for K^+ diffusion in the pore [10]. In this latter structure, a distance contraction in the KWKWKK sequence was observed, leading to a decrease of about 1 Å of the K_2–K_4 distance.

2. Methods

2.1. Molecular dynamics simulation

Our model system and simulation setup for the KcsA channel were described elsewhere [16]. Let us summarize the general method.

The structure was built on the basis of the 2.0 Å resolution closed 1K4C structure (see [22] for details). On the 534 aminoacids of the original structure, we only conserved the 412 residues mostly burried in the lipidic bilayer. Four K^+ ions were included, as well as 226 over 469 water molecules which were relevant to retain. Six aminoacid side chains were incomplete in the X-ray structure and the missing parts were added. All other aminoacids were perfectly well defined and their respective positions used as the starting MD configuration. The part of the protein ranging from Trp87 to Trp113 was immersed inside an octane slab of 29 Å thickness [23], the total volume of the box being approximately equal to 73 $Å^3$. On each side of the octane slab, a 22 $Å^3$ thickness slab of water molecules was appended, modeling the extra and intracellular hydration layers. All the water molecules were of TIP3P type.

The simulations were performed using AMBER suite of programs with AMBER 6 force field [17]. The total simulation time lasted about 1.4 ns. A time step of 1 fs was required to correctly take into account all external movements, including water rotations. Simulations were performed following the approach proposed by Bernèche and Roux [24].

2.2. Ab initio calculations

Merz–Kollman charges [18,19] were calculated using GAUSSIAN-03 [20] on a multiprocessor Compaq ALPHA machine. The computations were run at Hartree-Fock 6-31G(d) level of theory [25], without any further energy minimization, in order to be strictly consistent with the MD snapshot pictures, and without self-consistent reaction field switched on. Indeed, as this level exaggerates the dipole moment, this situation roughly corresponds to the polarized case. It is also a good compromise between accuracy of the results and computational time. One may recall at this point that atomic charges are not a quantum mechanical observable, unlike electron density, and their calculation is dependent on the model which is used. Direct experimental determination is thus impossible. However, Merz–Kollman–Singh population analysis was elaborated

by taking into account several molecular properties [26,27]. Moreover one specific geometry will always give perfectly reproducible results; no significant statistical error bar associated with each value can be drawn at the third decimal place, and one precise given geometry will always correspond to one unique set of results. K^+ ion radius input was 1.33 Å [4].

We chose to more specifically look at S_1 to S_4 sites, where were located respectively: one water molecule (W_1), a K^+ ion (K_2), a water molecule (W_3) and a K^+ ion (K_4). Therefore we truncated KcsA structure at the level of the four Tyr78 residues, where the peptide bond with Gly79 was cut and ended with a hydrogen (–CHO), and near the cavity below the four Thr74, –NH of the amide bond completed to NH_2. The sequence portion considered was thus (Thr74–Thr75–Val76–Gly77–Tyr78)$_4$ (Fig. 2). No lipidic or water environment constitutive of the MD construct was considered, and the total number of atoms was 304.

Two configurations of the selectivity filter were examined, namely C1 and C2: the geometry shown in Fig. 2a corresponds to the average configuration C1, whereas the one in Fig. 2b, C2, to the specific situation we could observe in the same trajectory. We clearly see that in the latter, the potassium ions and water molecules are no longer aligned with regard to the vertical central axis of the filter (see Section 3). The center to center distances between the K^+ and oxygens of the water molecules, as well as the K^+–K^+ distances for each configuration are indicated in Table 1.

Although partial charges may be affected by the truncation or the lack of a lipidic environment, modeled either by octane as was the case in our MD simulations or with a continuum dielectric medium, one may believe that the two K^+ ions and water molecules are buried enough within both structures not to be greatly affected, especially when comparing the two geometries. In the same way, an effect of the upper water hydration layer or the water molecules of the cavity could not be taken into account. Ideally, all the atoms of the system plus a real or modeled lipidic and aqueous environment should of course have been used for an accurate full quantum description of the selectivity filter window, but it would have been computationally unconceivable at this level of theory. We are convinced that this simplification is not irrelevant and that the effect of the direct environment on the charges nearby the two K^+ and two water molecules, and consequently the effect due to the difference in atom positions between both structures, is predominant.

3. Results and discussion

We report in Tables 1 and 2 the results of the MK charges computations for the oxygen atom of the two

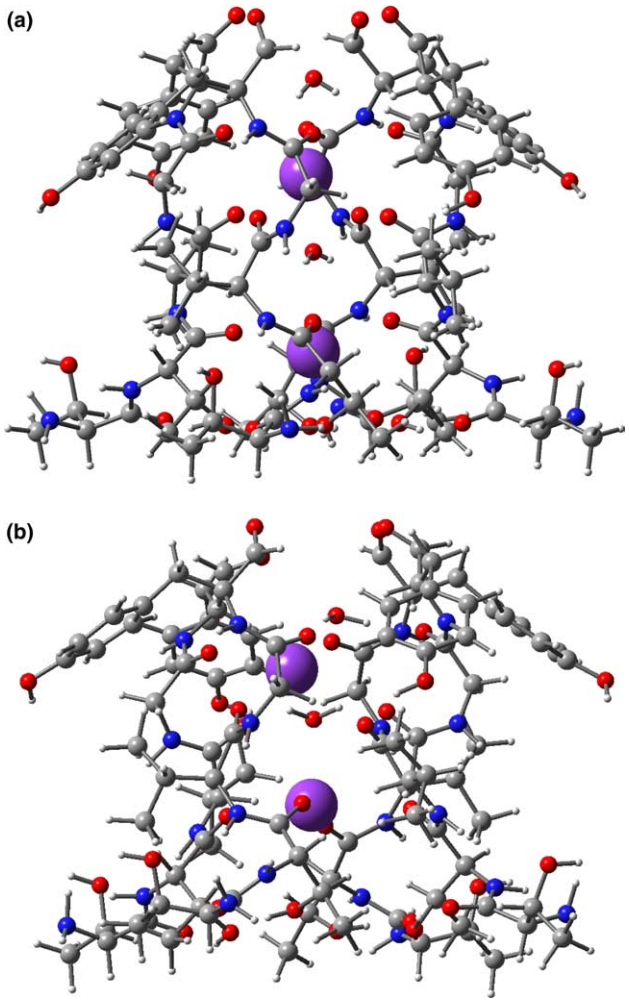

Fig. 2. Molecular model of the KcsA selectivity filter (Thr74 to Tyr78 truncated structure). (a) Average configuration over 600 ps MD. (b) Specific snapshot in the same trajectory suspected to be at the origin of the 'knock-on' mechanism. In the central vertical axis are disposed the two water molecules and the two K^+ ions of sites S_1 to S_4 (from top to bottom). For clarity, van der Waals radii are scaled by 40%. K^+ is shown in purple, oxygen in red, nitrogen in blue, carbon in dark grey and hydrogen in light grey.

water molecules, the two K^+ ions, the nitrogen, carbon and oxygen atoms of the 12 peptide bonds and the carbon and oxygen atoms of the CHOH part of the Thr74 lateral chain, for which oxygens are coordinated with the potassium, for both geometries. We clearly see in Table 1 that the ionic charge for the potassium is not +1, which is the fixed value usually taken in MD simulations, but can be as low as +0.687.

In the C2 situation (see [14] for a detailed description of the structure), to the contrary of the C1, the two water molecules' centers of mass are no longer along the vertical axis going through the K^+ ions, but off centered on the same side of the two K^+. The K^+–K^+ distance is decreased by about 1 Å, and the two water molecules get placed at the same level as the eight amide carbonyls around K_2, replacing on each side one of the

Table 1
Center to center distances (Å) between the oxygen atom of the water molecules and the K^+ ions of sites 1 to 4 of the KcsA selectivity filter (first data); second data (bold), MK partial charges in units of electron charge (e^-) for $O(H_2O)$ or K^+ of the corresponding sites

	$O(W_1)$–K_2	K_2–$O(W_3)$	$O(W_3)$–K_4	K_2–K_4
600 ps average geometry (C1)	3.10; **O: −0.767**	2.40; **O: −0.816**	3.05	5.35; **K_2: 0.755–K_4: 0.687**
Specific snapshot (C2)	2.68; **O: −0.876**	2.51; **O: −0.948**	2.79	4.30; **K_2: 0.871–K_4: 0.875**

Table 2
MK charges (e^-) of the nitrogens (first row), carbons and oxygens (second row) of the peptide bonds, and carbons and oxygens of the CHOH part of the Thr74 lateral chain, where oxygens are coordinated with K_2 and K_4, on each consecutive peptide (1st to 4th)

Peptide chain		1st	2nd	3rd	4th
Tyr78–Gly77 **N–C=O**	C1	−0.832	−0.659	−0.852	−0.708
		0.622/−0.624	0.456/−0.471	0.794/−0.674	0.523/−0.563
	C2	−0.910	−0.756	−0.808	−0.617
		0.785/−0.605	0.734/−0.636	0.794/−0.719	0.688/−0.667
Gly77–Val76 **N–C=O**	C1	−0.829	−0.903	−0.750	−0.944
		0.910/−0.457	1.019/−0.600	0.778/−0.479	**1.023/−0.573**
	C2	−0.735	−0.661	−0.565	−0.640
		0.902/−0.642	0.903/−0.610	1.022/−0.539	**0.491/−0.501**
Val76–Thr75 **N–C=O**	C1	***−0.333***	***−0.560***	***−0.967***	***−0.535***
		0.590/−0.491	0.716/−0.525	**0.915/−0.521**	0.715/−0.544
	C2	***0.049***	***−0.026***	***−0.008***	***−0.362***
		0.289/−0.565	0.494/−0.561	**0.565/−0.577**	0.659/−0.629
Thr74 **CHOH**	C1	0.810/−0.929	0.822/−0.868	1.171/−0.952	0.790/−0.724
	C2	0.567/−0.798	0.959/−0.810	1.052/−0.898	0.790/−0.861

carbonyls' coordinations. Moreover, K_4 gets about aligned in the center of the carbonyl ring which is located above in the average situation, distancing itself from its bottom threonine OH interactions. It is thus moving closer to the water/carbonyls ring sitting above, sharing together with the other potassium more interactions with this layer than with the OH's ring.

These different atomic positions and distance contributions are reflected in the corresponding charge distributions. In the C2 geometry, MK charges for the water oxygens and K_2 ion are increased by more than 0.1 e^- in absolute value with regard to C1, whereas an increase of about 0.19 e^- is obtained for K_4, which is a consequent change in the charge (Table 1).

One may attribute the observed variation of these reported MK charges to the well-known buried atom problem. Indeed, in the MK method, charges are fitted to the electrostatic potential (ESP) sampled around the van der Waals surface of the molecule. A short-coming of this procedure is that atoms that are not close to this surface have a small influence on the ESP on the surface. As a consequence they may not be accurately determined since they can vary very much without affecting the goodness of the fit significantly [28]. This nevertheless does not seem to be the case here for mainly two reasons (Konrad Hinsen, private communication): (i) if one sums up the charges of the ions and their nearest neighbors, then this sum varies much more when comparing C1 to C2 than the corresponding charge on the potassium ions. For instance on K_2 site, considering the eight carbonyls of the surrounding amide bonds plus the two water molecules, this leads to a variation of 0.35 e^- for the sum, while only −0.12 e^- is found for the K^+ variation; (ii) the MK charges obtained for the two water molecules in the filter are rather close to the TIP3P or SPC models of charge commonly used in molecular dynamics force fields (−0.834 [29] or −0.820 [30] for the oxygen atom, respectively). This latter observation reinforces the physical meaning of the MK charges that we determined for the potassium, since the same numerical problem could as well appear on the water molecules, which again does not look to be the case. We envisage to perform a more sophisticated but systematic approach for the validation of these MK partial charges by using a method based on singular value decomposition, described by Hinsen and Roux [31] in an application for the study of proton transfer in acetylacetone, and e.g. used by Carey et al. [28] for improving ESP charges for sugars.

The differences on the N–C=O's and the CHOH's are more difficult to apprehend but, as one can see in Table 2, they may be as important as C1 (0.915, −0.521) to C2 (0.565, −0.577) for one of the C=O's of Val76–Thr75 peptide bond, which represents a Δe^- for the carbon of 0.35, or C1 (1.023, −0.573) to C2 (0.491, −0.501) for one of the C=O's of Gly77–Val76 peptide bond,

which for the carbon is a Δe^- of about 0.53 (bold, Table 2).

Parallely in the same ring, charge values may vary the opposite way or remain about the same. Whereas charges remain relatively unaffected for the Tyr78–Gly77 N–C=O's, as well as for the Thr74 CHOH's (even though one of the CHOH's gets very polarized, in the 3rd peptide), the situation is indeed very different for the Gly77–Val76 and Val76–Thr75 N–C=O's. A surprising feature to be noticed throughout Table 2 is that all the oxygen atoms, even where the carbonyl carbons get highly charged, remain relatively constant in charge: -0.57 ± 0.14 e^- for the C=O's, -0.85 ± 0.13 e^- for the CHOH's. The big difference between C=O's and CHOH's oxygen mean charge values may be due to a stronger delocalization of the charge on the C=O's towards the potassium, which becomes less positive. This looks to be particularly the case for K_4 in C1 (0.687 e^-), whereas K_4 in C2 is closer to 1 e^- being also closer to K_2 and further away from the bottom CHOH's (Fig. 2b). If we further consider the nitrogen atoms of the three peptide bond rings, we observe that the charges become strikingly close to zero in the C2 configuration, except for the 4th peptide (italic/bold, Table 2). Although the distances between K_4 and the Val76–Thr75 amide bond oxygens are shorter and less dispersed in C1 (2.50 ± 0.05 Å) than in C2 (2.80 ± 0.32 Å), the nearly in plane position of C2 K^+ with regard to these C=O's may explain such distinctive values on the nitrogen charges. Thus, the ('soft') K^+/('hard') oxygens coordination geometry is important to consider as for the specific charge transfers towards neighbor atoms. If one wants to look at the symmetry of the distribution of partial charges at the level of the different N–C=O or CHOH rings (Δe^- (1st/3rd peptide) vs. Δe^- (2nd/4th peptide)), it can be noticed that for the nitrogens, charges are rather symmetrical except Δe^- (1st/3rd peptide) in C1 ($\Delta e^- = 0.63$), and Δe^- (2nd/4th peptide) in C2 ($\Delta e^- = 0.34$) for Val76–Thr75 around K_4. For the carbons, the overall differences are more distributed, with Δe^- (1st/3rd peptide) = 0.32 (C1) and 0.28 (C2) for Val76–Thr75, 0.36 (C1) and 0.48 (C2) for Thr74, and Δe^- (2nd/4th peptide) = 0.41 for Gly77–Val76.

All in all, general trends regarding such charge differences based on distance and angle analysis are not obvious to find. Subtile charge transfers may occur, possibly propagating along the peptide backbones and residues up to several atomic positions from a given partial point charge influence [32]. Moreover, some extreme values of the MK charges might adjust through further energy minimization of the geometry in a whole self-consistent ab initio calculation. Nevertheless the present charge analysis on the basis of these two C1 and C2 situations gives an idea of the differences possible to occur.

4. Conclusion

In these ab initio investigations of the KcsA selectivity filter, we point out significant differences in MK partial charges, putting under question mark the application of effectively polarized force fields. Indeed, potassium charges show to be very sensitive to the filter local environment, especially their specific position with regard to the carbonyls of the peptide bonds they are coordinated to, the hydroxyls of the Thr74 in the case of K_4 or the water molecules. Our results show that the mechanism of the potassium ions transport through the KcsA pore would deserve to be revisited by considering more realistic polarizable force fields, looking as well at the flowing water and ions as at the electron transfer along the peptide chains, the whole functioning as a tight reactive charge relay system. The lower value obtained for the charge on the two K^+ ions compared to the +1 charge used in usual force fields might certainly favour their diffusion through the pore, since the attractive electrostatic interactions between the protein and the ions will decrease. In a further step, similar ab initio calculations will be performed to investigate the entire filter ion permeation mechanistics.

We feel that within the next decade the effectively polarized force field for biomolecular simulation will be gradually replaced by electronically polarizable models [33]. Point polarizabilities and shell polarizabilities are possible practical implementations [34]. On the other hand, inclusion of electron transfer effects to applied force fields are not demanding. Application of computationally tractable quantum mechanics/molecular mechanics (QM/MM) methods like empirical valence bond (EVB) methodology [35] seems to be the only possible way to include such effects. Charge transfers are of special importance for ions with a high charge, like Ca^{2+}, or when an ion is transferred from aqueous solution to less polar environment, or from one site to the other in a channel protein as was the case in our study.

The common argument for application of effectively polarized force fields, i.e. that this effect is absorbed in the Lennard–Jones part of the intermolecular interaction, becomes questionable in such cases. All in all, we believe that there is plenty of room for force field development for the ions in the context of polarizability and charge transfer effects.

Acknowledgements

P.H. wishes to thank the Ligue du Doubs contre le Cancer of France for financial support. M.C. is grateful to Professor P. Carloni for computer facilities in SISSA (Trieste, Italy).

References

[1] M.S.P. Sansom, I.H. Shrivastava, J.N. Bright, J. Tate, C.E. Capener, P.C. Biggin, Biochim. et Biophys. Acta 1565 (2002) 294.
[2] G. Yellen, Nature 419 (2002) 35.
[3] J. Tamargo, R. Caballero, R. Gómez, C. Valenzuela, E. Delpón, Cardiovasc. Res. 62 (2004) 9.
[4] D.A. Doyle, J.M. Cabral, A. Pfuetzner, A. Kuo, J.M. Gulbis, S.L. Cohen, B.T. Chait, R. MacKinnon, Science 280 (1998) 69.
[5] L. Guidoni, V. Torre, P. Carloni, Biochemistry 38 (1999) 8599.
[6] P.C. Biggin, G.R. Smith, I. Shrivastava, S. Choe, M.S.P. Sansom, Biochim. et Biophys. Acta 1510 (2001) 1.
[7] I.H. Shrivastava, D.P. Tieleman, P.C. Biggin, M.S.P. Sansom, Biophys. J. 83 (2002) 633.
[8] J.H. Morais-Cabral, Y. Zhou, R. MacKinnon, Nature 414 (2001) 37.
[9] B. Roux, S. Bernèche, W. Im, Biochemistry 39 (2000) 13295.
[10] S. Bernèche, B. Roux, Nature 414 (2001) 73.
[11] L. Guidoni, P. Carloni, Biochim. et Biophys. Acta 1563 (2002) 1.
[12] V.B. Luzhkov, J. Åqvist, Biochim. et Biophys. Acta 1481 (2000) 360.
[13] Y.-S. Liu, P. Sompornpisut, E. Perozo, Nature Struct. Biol. 8 (2001) 883.
[14] Y. Jiang, A. Lee, J. Chen, M. Cadene, B.T. Chait, R. MacKinnon, Nature 417 (2002) 523.
[15] L. Guidoni, V. Torre, P. Carloni, FEBS Lett. 477 (2000) 37.
[16] M. Compoint, P. Carloni, C. Ramseyer, C. Girardet, Biochim. et Biophys. Acta 1661 (2004) 26.
[17] D.A. Case et al., AMBER 6, University of California, San Francisco, 1999.
[18] B.H. Besler, K.M. Merz Jr., P.A. Kollman, J. Comput. Chem. 11 (1990) 431.
[19] U.C. Singh, P.A. Kollman, J. Comput. Chem. 5 (1984) 129.
[20] M.J. Frisch et al., GAUSSIAN-03, Revision B.03, Gaussian Inc., Pittsburgh PA, 2003.
[21] A.L. Hodgkin, R.D. Keynes, J. Physiol. 128 (1955) 61.
[22] Y. Zhou, J.H. Morais-Cabral, A. Kaufman, R. MacKinnon, Nature 414 (2001) 43.
[23] C.E. Capener, M.S.P. Sansom, J. Phys. Chem. B 106 (2002) 4543.
[24] S. Bernèche, B. Roux, Biophys. J. 78 (2000) 2900.
[25] J.B. Foresman, A. Frisch, Exploring Chemistry with Electronic Structure Methods, second ed., Gaussian Inc., Pittsburgh, PA, 1996.
[26] U.C. Singh, P.A. Kollman, J. Comput. Chem. 5 (1984) 129.
[27] S.R. Cox, D.E. Williams, J. Comput. Chem. 2 (1981) 304.
[28] C. Carey, L.E. Chirlian, M.M. Francl, D.M. Gange, Glycoconj. J. 14 (1997) 501.
[29] W.L. Jorgensen, J. Chandrasekhar, J.D. Madura, R.W. Impey, M.L. Klein, J. Chem. Phys. 79 (1983) 926.
[30] H.J.C. Berendsen, J.P.M. Postma, W.F. van Gunsteren, J. Hermans, in: B. Pullman (Ed.), Intermolecular Forces, Reidel, Dordrecht, 1981, p. 331.
[31] K. Hinsen, B. Roux, J. Comput. Chem. 18 (1997) 368.
[32] P. Huetz, C. Ramseyer, C. Girardet, Chem. Phys. Lett. 380 (2003) 424.
[33] A.D. Mackerell Jr, M. Feig, C.L. Brooks 3rd, J. Comput. Chem. 25 (2004) 1400.
[34] P.C. Jordan, P.J. van Maaren, J. Mavri, D. van der Spoel, H.J.C. Berendsen, J. Chem. Phys. 103 (1995) 2272.
[35] A. Warshel, W.W. Parson, Q. Rev. Biophys. 34 (2001) 563.